Supplementary Information (SI) for Journal of Materials Chemistry C.

Supporting Information for

Adaptive Self-powered Photodetection and Neuromorphic Computing in $CuCrP_2S_6$ Ionotronic Device

Yanan Cao[1,#], Wan Wang[1,2,#], Jiao Peng[3,#], Xin Chen[1,2], Yezhao Zhuang[2], Bo Peng[2], Lu Cheng[4], Zhipeng Zhong[2], Jianlin Shi[2], Xiang Li[2], Wu Shi[5], Jianlu Wang[2], Junhao Chu[2], Hai Huang[2*]

[1] *State Key Laboratory of Digital Intelligent Technology for Unmanned Coal Mining, Anhui University of Science and Technology, Huainan 232001, China*

[2] *State Key Laboratory of Photovoltaic Science and Technology, Shanghai Frontiers Science Research Base of Intelligent Optoelectronic and Perception, Institute of Optoelectronics and College of Smart Materials and Future Energy, Fudan University, Shanghai 200433, China*

[3] *West Anhui University, Lu'an, Anhui 237012, China*

[4] *Institute of Biomedicine, University of Eastern Finland, Kuopio, 70210, Finland*

[5] *State Key Laboratory of Surface Physics and Institute for nanoelectronic devices and quantum computing, Fudan University, Shanghai 200433, China*

[#] These authors contributed equally.

[*] Correspondence to: Hai Huang (huangh@fudan.edu.cn)

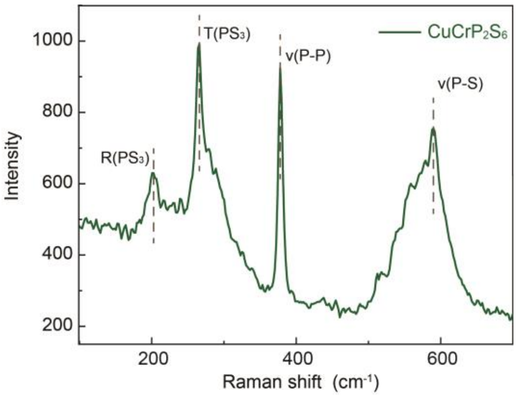

Figure S1. Raman spectrum of CCPS nanoflake.

Raman spectrum of the CCPS sample acquired using a confocal Raman microscope (inVia Qontor, Renishaw) with 532 nm laser excitation. The peaks at 204 and 266 cm^{-1} are attributed to the rotational and translational modes of the PS_3 group, while those at 378 and 591 cm^{-1} correspond to the out-of-plane vibrations of the P–P and P–S bonds, respectively.

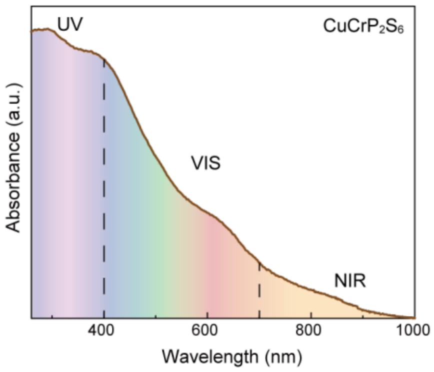

Figure S2. Ultraviolet-Visible-Near infrared photon absorption spectrum of CCPS nanoflakes ranging from 250 to 1000 nm.

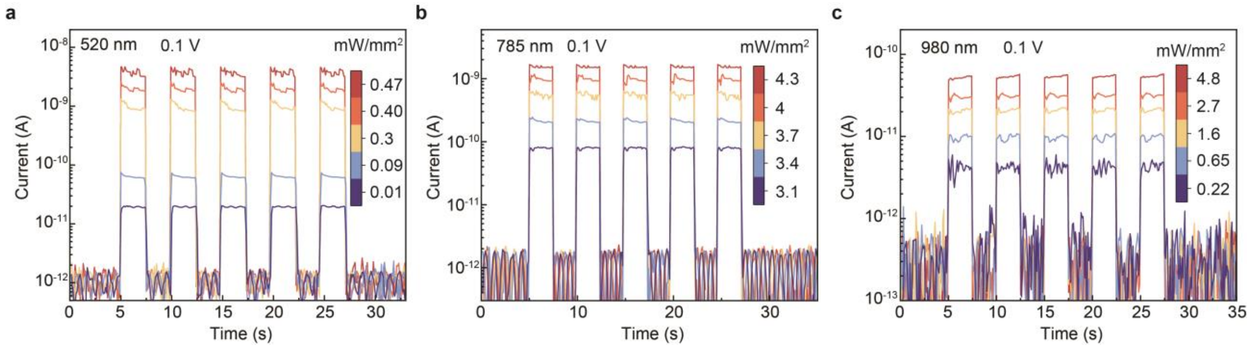

Figure S3. Time resolved photoresponse of the CCPS photodetector to 520 nm (a), 785 nm (b) and 980 nm (c) light with varying intensities.

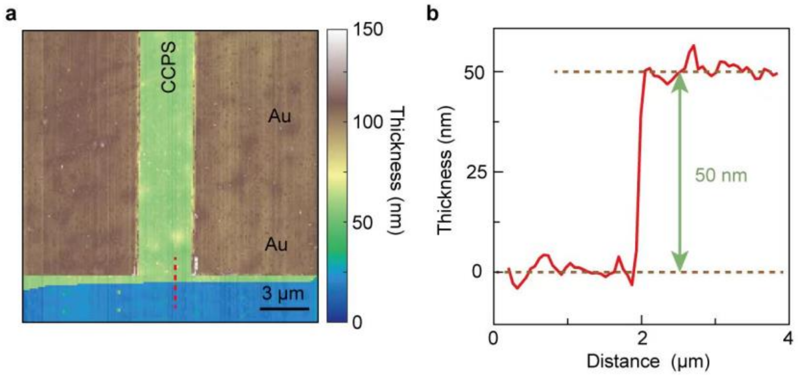

Figure S4. The in-plane two terminal device structure of $CuCrP_2S_6$ measured through atomic force microscopy. (a) AFM tomography of the CCPS device. (b) The thickness profile of the CCPS nanoflake.

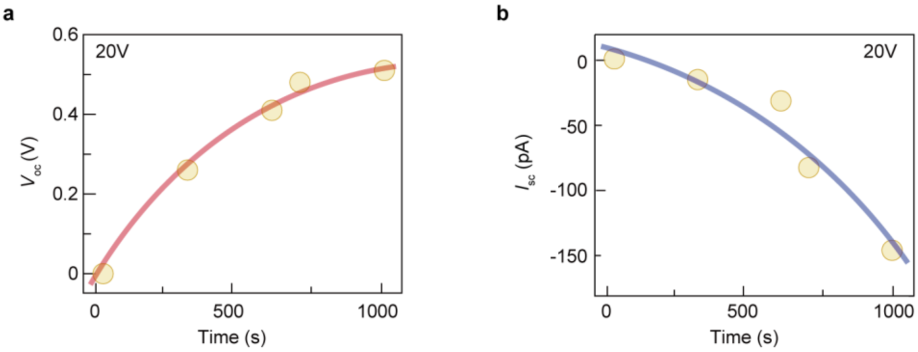

Figure S5. Open-circuit voltage and short-circuit current under 20V bias with varying durations. **(a)** Open-circuit voltage after applying 20 V bias with duration from 0 to 1000 s. **(b)** Short-circuit current after applying 20 V bias with duration from 0 to 1000 s.

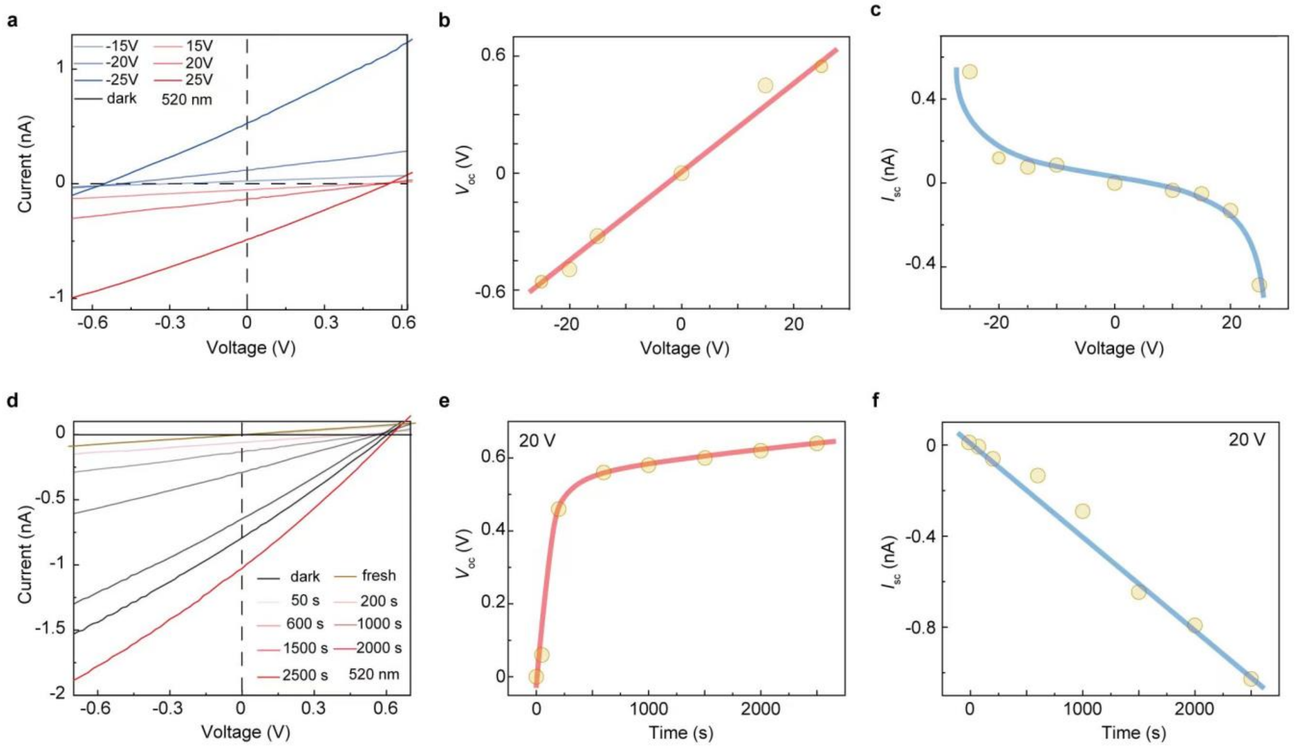

Figure S6. *I–V* curves of the CCPS device for 520 nm light after applying various voltages conditions. (a) *I-V* curves of the CCPS device under 520 nm after applying different bias voltages with the same duration. **(b, c)** The extracted V_{oc} and I_{sc} after applying varying bias voltages. **(d)** *I-V* curves of the CCPS device under 520 nm after applying 20 V voltage with duration from 0 to 2500 s. **(e, f)** The extracted V_{oc} and I_{sc} after applying 20 V for varying duration.

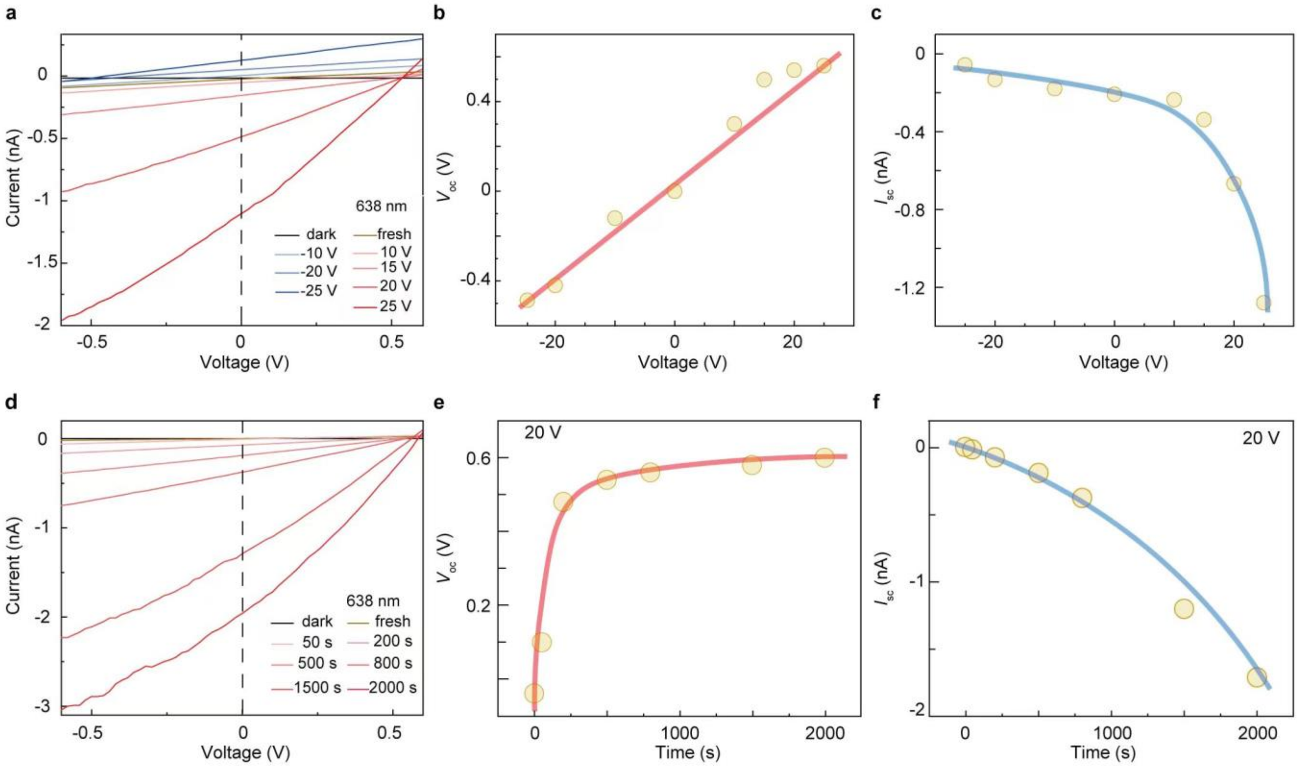

Figure S7. *I*–*V* curves of the CCPS device for 638 nm light after applying various voltages conditions. (a) *I-V* curves of the CCPS device under 638 nm after applying different bias voltages with the same duration. **(b, c)** The extracted V_{oc} and I_{sc} after applying varying bias voltages. **(d)** *I-V* curves of the CCPS device under 638 nm after applying 20 V voltage with duration from 0 to 2000 s. **(e, f)** The extracted V_{oc} and I_{sc} after applying 20 V for varying duration.

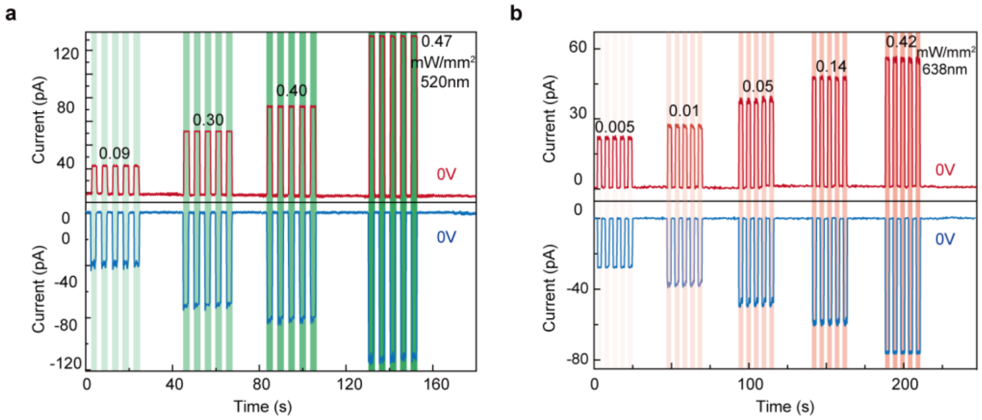

Figure S8. Photovoltaic response of the CCPS device under 520 nm and 638 nm with varying light intensities. (a, b) Time-resolved photocurrent of the CCPS device under 520 nm (a) and 638 nm (b) illumination with varying light intensities at 0 V bias voltage after driven the ions to opposite directions, resulting in photocurrent reversal.

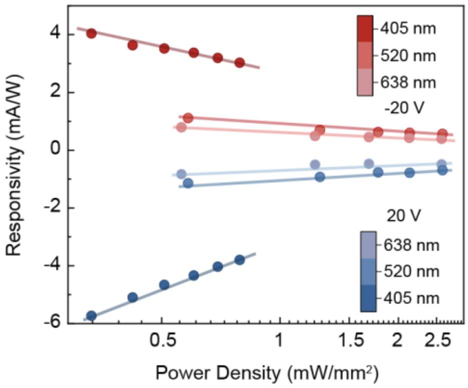

Figure S9. Responsivity of CCPS self-powered photodetectors under opposite polarity bias modulation.

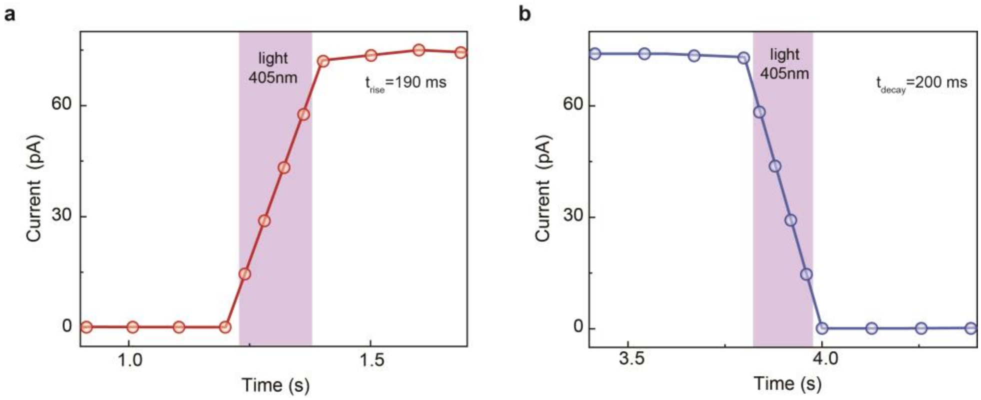

Figure S10. Response time of the CCPS self-driven photodetector. (a-b) Rising edge and falling edge of the self-powered $CuCrP_2S_6$ photodetector for 405 nm light.

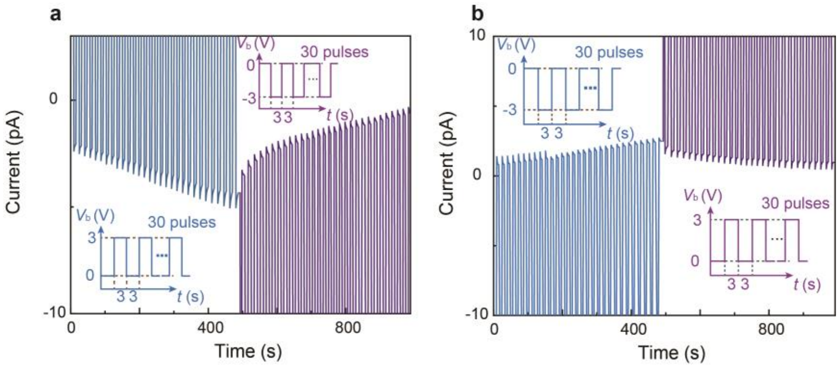

Figure S11. Long-term potentiation (LTP) and long-term depression (LTD) curves under opposite polarity bias modulation. (a) LTP and LTD processes under positive bias modulation (LTP: writing voltage 3 V, reading voltage 0 V; LTD: erasing voltage -3 V, reading voltage 0 V). **(b)** LTP and LTD processes under negative bias modulation (LTP: writing voltage -3 V, reading voltage 0 V; LTD: erasing voltage 3 V, reading voltage 0 V).

The photovoltaic current of CCPS device was modulated by applying a bias, where the built-in electric field direction opposes the applied bias. At a reading voltage of 0 V, the device exhibits a positive open-circuit voltage and a negative short-circuit current. Then, under 0 V reading bias, the device is illuminated with a 405 nm laser at a light power density of 0.5 mW/mm^2. As the number of electric pulses increases, the short-circuit current at 0 V gradually increases, demonstrating reverse long-term potentiation (LTP). Subsequently, applying -3 V suppressive voltage causes the short-circuit current to gradually decrease with increasing light pulses, showing reverse long-term depression (LTD).

When CCPS is modulated by applying a negative bias, the device exhibits the opposite behavior, showing forward LTP and LTD.

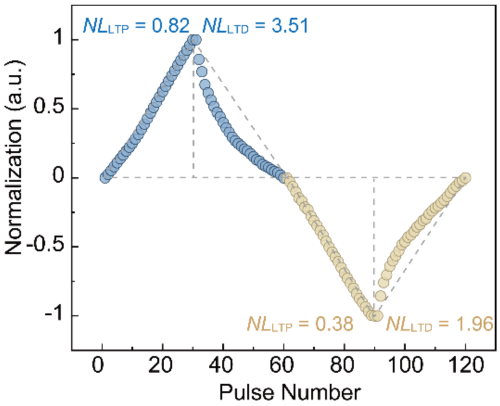

Figure S12. The nonlinearity of long-term potentiation (LTP) and long-term depression (LTD).

$$G_{\mathrm{LTP}} = B\left(1-e^{-\frac{P}{A}}\right) + G_{\min} \tag{1}$$

$$G_{\mathrm{LTD}} = -B\left(1-e^{-\frac{P-P_{\max}}{A}}\right) + G_{\max} \tag{2}$$

$$B = (G_{\max} - G_{\min})/\left(1-e^{\frac{-P_{\max}}{A}}\right) \tag{3}$$

Where G_{LTP} and G_{LTD} denote the responsivity values corresponding to the LTP and LTD curves, respectively. $G_{\min}$ and $G_{\max}$ represent the minimum and maximum responsivity values. P is the number of applied programming pulses, and $P_{\max}$ denotes the maximum pulse number. The parameter A characterizes the degree of nonlinearity in the LTP/LTD curves. The fitting procedure was performed using the MATLAB platform.

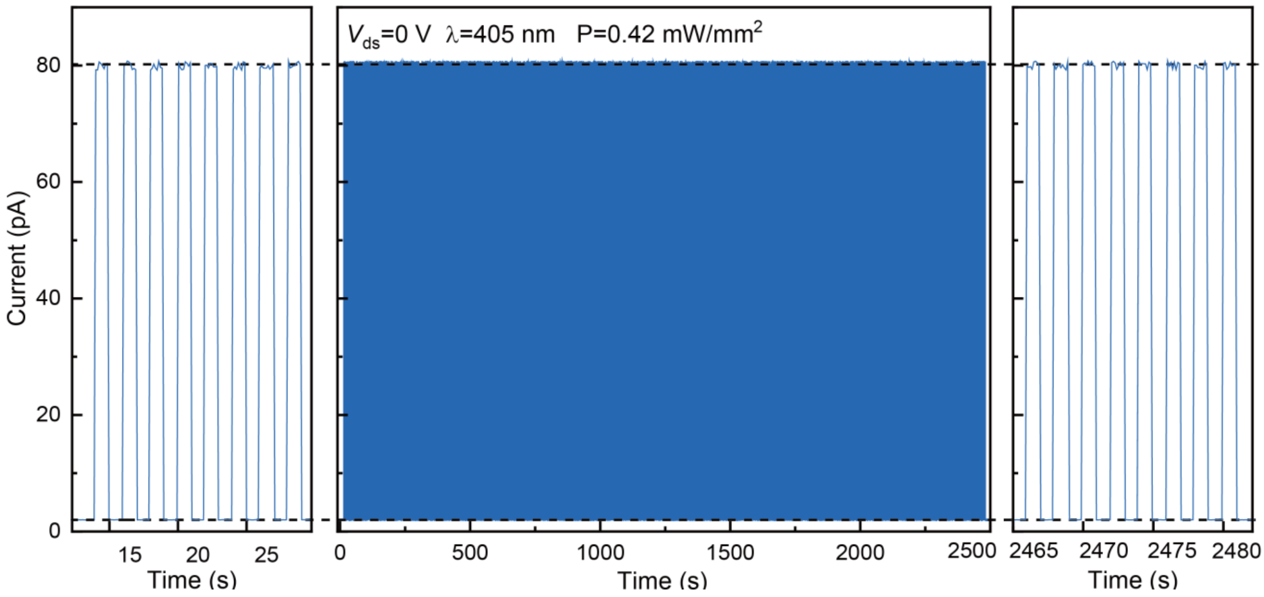

Figure S13. The self-driven photovoltaic response of CCPS homojunction. The photoresponse of 405 nm (P = 0.42 mW/mm^2) is achieved by internal-built electric field in CCPS device with 0 V external bias. This photovoltaic response is stable and maintains for 1200 cycles.

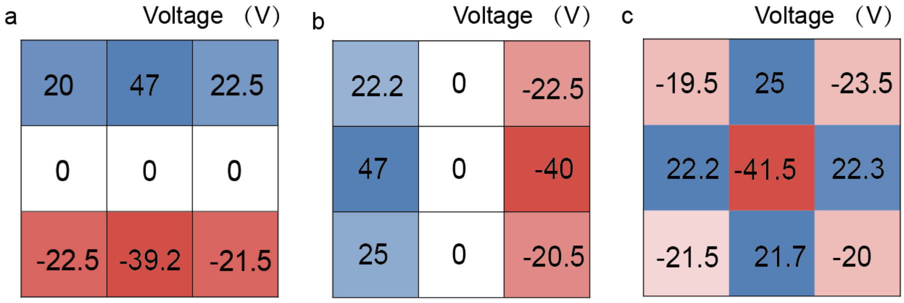

20	47	22.5
0	0	0
-22.5	-39.2	-21.5

22.2	0	-22.5
47	0	-40
25	0	-20.5

-19.5	25	-23.5
22.2	-41.5	22.3
-21.5	21.7	-20

Figure S14. Programming voltages for horizontal, vertical, and sharpening convolutional kernels. (a) Programming voltages for constructing the vertical convolutional kernel array with a modulation time of 580 s. (b) Programming voltages for constructing the horizontal convolutional kernel array with a modulation time of 580 s. (c) Programming voltages for constructing the sharpening convolutional kernel array with a modulation time of 580 s.